

LETTER • OPEN ACCESS

Vegetation disturbances characterization in the Tibetan Plateau from 1986 to 2018 using Landsat time series and field observations

To cite this article: Yanyu Wang *et al* 2023 *Environ. Res. Lett.* **18** 014016

View the [article online](#) for updates and enhancements.

You may also like

- [THE INSIDIOUS BOOSTING OF THERMALLY PULSING ASYMPTOTIC GIANT BRANCH STARS IN INTERMEDIATE-AGE MAGELLANIC CLOUD CLUSTERS](#)

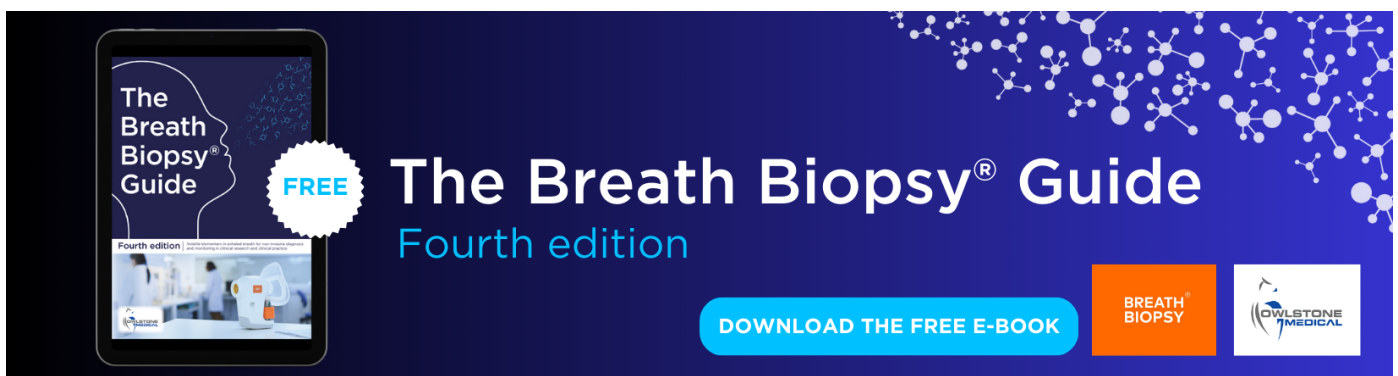
Léo Girardi, Paola Marigo, Alessandro Bressan *et al.*

- [THE CONTRIBUTION OF TP-AGB AND RHeB STARS TO THE NEAR-IR LUMINOSITY OF LOCAL GALAXIES: IMPLICATIONS FOR STELLAR MASS MEASUREMENTS OF HIGH-REDSHIFT GALAXIES](#)

J. Melbourne, Benjamin F. Williams, Julianne J. Dalcanton *et al.*

- [Mapping the temporal pole with a specialized electrode array: technique and preliminary results](#)

Taylor J Abel, Ariane E Rhone, Kirill V Nourski *et al.*



The Breath Biopsy® Guide
Fourth edition

FREE

DOWNLOAD THE FREE E-BOOK

BREATH BIOPSY

OWLSTONE MEDICAL

ENVIRONMENTAL RESEARCH
LETTERS

LETTER

OPEN ACCESS

RECEIVED
1 September 2022REVISED
9 December 2022ACCEPTED FOR PUBLICATION
13 December 2022PUBLISHED
3 January 2023

Original content from
this work may be used
under the terms of the
[Creative Commons
Attribution 4.0 licence](#).

Any further distribution
of this work must
maintain attribution to
the author(s) and the title
of the work, journal
citation and DOI.

Vegetation disturbances characterization in the Tibetan Plateau
from 1986 to 2018 using Landsat time series and field
observationsYanyu Wang¹, Ziqiang Ma², Yuhong He³, Wu Yu^{1,4}, Jinfeng Chang¹, Dailiang Peng⁵, Xiaoxiao Min¹,
Hancheng Guo¹, Yi Xiao¹, Lingfang Gao¹ and Zhou Shi^{1,6,*}¹ Institute of Agricultural Remote Sensing and Information Technology Application, College of Environmental and Resource Sciences, Zhejiang University, Hangzhou 310058, People's Republic of China² Institute of Remote Sensing and Geographical Information Systems, School of Earth and Space Sciences, Peking University, Beijing 100871, People's Republic of China³ Department of Geography, Geomatics and Environment, University of Toronto Mississauga, Mississauga, ON L5L 1C6, Canada⁴ College of Resource and Environment, Tibet University, Nyingchi 860000, People's Republic of China⁵ Key Laboratory of Digital Earth Science, Aerospace Information Research Institute, Chinese Academy of Sciences, Beijing 100094, People's Republic of China⁶ State Key Laboratory of Soil and Sustainable Agriculture, Institute of Soil Science, Chinese Academy of Sciences, Nanjing 210008, People's Republic of China

* Author to whom any correspondence should be addressed.

E-mail: shizhou@zju.edu.cn**Keywords:** disturbance, vegetation, change detection, time series, Landsat, Tibetan PlateauSupplementary material for this article is available [online](#)**Abstract**

Disturbances in vegetated land could dramatically affect the process of vegetation growth and reshape the land cover state. The overall greenup of vegetation on the Tibetan Plateau (TP) has almost served as a consensus to date. However, we still lack consistent acquisitions on the timing, the spatial patterns, and the temporal frequency of vegetation disturbance over the TP, limiting the capacity for planning land management strategies. Therefore, we explored the spatiotemporal pattern and variation of vegetation disturbances across the TP during the past decades and analyzed the disturbance agents. We utilized 37-year Landsat time series images and field observations coupled with a temporal segmentation approach to characterize the spatiotemporal pattern of vegetation disturbances across the TP for the period 1986–2018. The results from this study revealed that 75.71 M ha (accounting for 29.34% of TP's area) vegetation area underwent at least one disturbance, of which 8.44 M ha area ever experienced large-scale disturbances (disturbance area greater than 0.9 ha and disturbance magnitude (the difference between the spectral value of pre-disturbance and that of post-disturbance) over 0.2). Further, the spatial distributions of these large-scale disturbances varied over time: before 2002, the disturbed sites were evenly distributed over the southeast part of the TP probably induced by overgrazing and unscientific livestock management, while after 2002, most disturbances were concentrated in the south of the Yarlung Tsangpo, mainly caused by anthropogenic activities, such as urban area, roadways, railway, and water control projects. This study presents an effort to characterize vegetation disturbances and their variations over the past decades on the TP, which provides crucial insights toward a complete understanding of vegetation dynamics and its causal relationship with human activities.

1. Introduction

As an integral part of the terrestrial ecosystem, vegetation regulates the exchange of carbon, water, impetus, and energy between the earth's surface and the

atmosphere (Bonan *et al* 1992, Haberl *et al* 2007). Change in vegetation structure and function could infer the effects of climate change and human interventions because vegetation is highly sensitive to various natural and anthropogenic factors (Parmesan and

Yohe 2003). To tackle urgent issues related to global climate change, carbon emissions and losses of biodiversity, detailed information about long-term vegetation dynamics over a large spatial extent and a long temporal scale is urgently needed (Dixon *et al* 1994, DeFries *et al* 1999, Brun *et al* 2019, Chen *et al* 2021, Smith *et al* 2022). In the past several decades, considerable attention has been dedicated to the changes in vegetation at regional to global scales using forest inventory and satellite observation data (Hansen *et al* 2013, Ceccherini *et al* 2020, Piao *et al* 2020). However, most of these only focused on the long-lasting trend of vegetation growth, lacking more detailed depiction of the inter-annual and intra-annual changes in vegetation, especially for the disturbance change within them (Verbesselt *et al* 2010, Watts and Laffan 2014). Referring to other related studies (Verbesselt *et al* 2010, Zhu *et al* 2020), we define the vegetation disturbance as the abrupt change where there is a significant decrease in vegetation volume within vegetated land caused by anthropogenic or natural processes. Vegetation disturbances caused by logging, urbanization, and fire could potentially alter the process of vegetation growth and affect local ecosystems. Accurate detection of such changes and attribution to the causes are therefore crucial for ecosystem management, biodiversity protection, and conservation policies (Krawchuk *et al* 2020, Ye *et al* 2021b).

The Tibetan Plateau (TP), referred to as the Earth's 'Third Pole', is one of the most vulnerable areas under global climate change. Over the past decades, a series of studies have investigated and revealed the trend of vegetation greening in the TP (e.g. Shen *et al* 2015a, Zhu *et al* 2016). Climate change, particularly the warming (Qiu 2008) and wetting (Chen *et al* 2013) trends, are thought to driving the long-term greening tendency of the vegetation on the TP (Piao *et al* 2014, Zhu *et al* 2016). Nevertheless, detailed information on inter-annual vegetation fluctuation was often ignored from the general greening trend in these previous studies (Piao *et al* 2011). The disturbance change of vegetation is a significant source of the inter-annual fluctuations especially for the ecological fragile zones like the TP. In recent years, the TP has suffered from more and more vegetation disturbance such as fire, overstocking (Harris 2010), active rodents (Yang *et al* 2017), increasing attention has therefore been paid on this regard. However, most of the previous studies were developed at a local scale or based on field observations (Qin *et al* 2014). Few studies have attempted to comprehensively characterize the disturbance-driven changes in vegetation over the TP with regards to their timing, duration, frequencies, and intensity.

Over the past decades, remote sensing technology has been highly sought after and found wide applications in terrestrial observation. Specifically, free and open access to the Landsat archive from 2008 has unlocked the critical bottleneck to the cost

and access to imagery, which has changed the way towards exploring the planet (Banskota *et al* 2014, Wulder *et al* 2019). Moreover, the dense time series image stacks have paved the way for a seamless detection of vegetation disturbances at an annual time step (Hansen *et al* 2013). Accordingly, various tools and algorithms have been proposed for monitoring vegetation change based on the Landsat time series, including offline change detection (e.g. Huang *et al* 2010, Kennedy *et al* 2010), online change detection (e.g. Verbesselt *et al* 2010, Zhu and Woodcock 2014), and ensemble strategy (e.g. Healey *et al* 2018, Bullock *et al* 2020). However, most related studies are focused on forest disturbances detection (Hansen *et al* 2016, Shimizu *et al* 2017, Senf and Seidl 2020, Ye *et al* 2021a), with fewer investigations conducted for vegetation disturbances, especially that occurring in mountainous areas.

We investigate the spatiotemporal characterization of vegetation disturbance of the TP from 1986–2018 for improving knowledge of the impact of human and natural coupled disturbances on the TP's vegetation. Specifically, the aims of this study were to: (a) detect the spatial-temporal characteristics of multiple vegetation disturbance and the inter-annual change of disturbed area for the study period; (b) analyze disturbance-driven vegetation changes among different vegetation types; (c) investigate the potential agents of vegetation disturbance change.

2. Materials and methods

The overall workflow of study is delivered in figure S1 (SI appendix), which consists of imagery preprocessing, index selection, time-series segmentation, and disturbance mapping.

2.1. Image data sets and preprocessing

A time series surface reflectance collection of Tier 1 Landsat 4, 5, 7, and 8 images during the period from 1984 to 2020 were employed in the study (1986–2018 for the actual detected years because no disturbances were mapped for the years 1984–1985 and 2019–2020, as current approach is unable to detect the disturbances in the beginning and end of the period). We only selected images within the plant growing season (from early May through middle September, SI appendix, figure S2) to minimize the influence of ice and snow and guarantee inter-annual spectral comparability of surface independent of phenological stages (Shen *et al* 2015b). Pixels with clouds and cloud shadows were masked out from all images utilizing the Fmask algorithm (Zhu and Woodcock 2014). To assure the inter-sensing harmonization and temporal continuity between Landsat sensors, we also conducted spectral transformation between Operational Land Imager and Enhanced Thematic Mapper Plus (ETM+) using the coefficients suggested by Roy

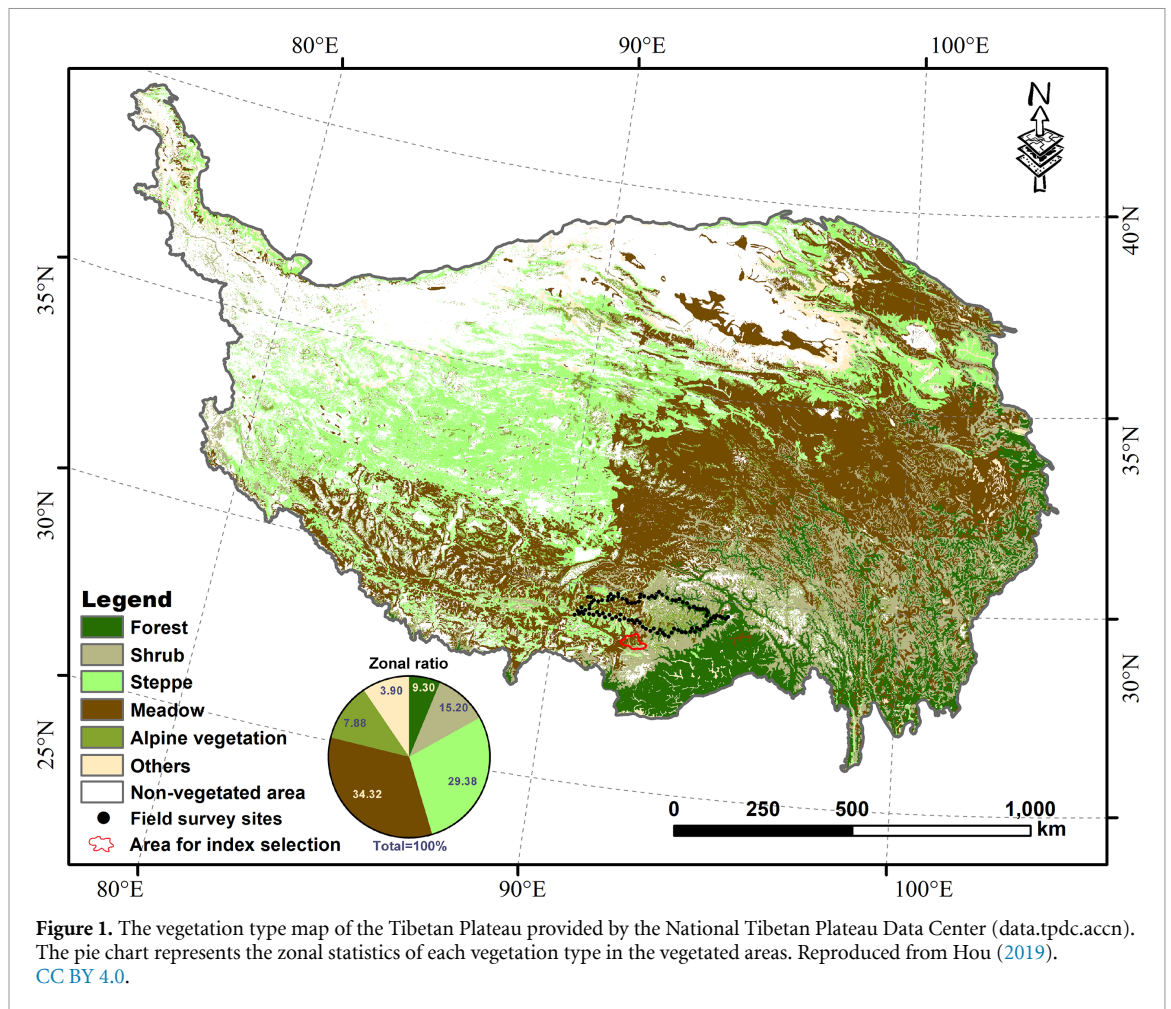


Figure 1. The vegetation type map of the Tibetan Plateau provided by the National Tibetan Plateau Data Center (data.tpdc.ac.cn). The pie chart represents the zonal statistics of each vegetation type in the vegetated areas. Reproduced from Hou (2019). CC BY 4.0.

et al (2016). Images were merged into annual composites using the medoid composites method, which is robust against extreme values and more efficient at generating value that is representative of the time series than the commonly used maximum composite method (Flood 2013). The preprocessing of the images was achieved with the help of Google Earth Engine.

To obtain the distribution characteristics of vegetation disturbance on the TP, we also used a vegetation map (Hou 2019). According to the vegetation map, we have divided five vegetation categories, including forest, steppe, meadow, shrub, and alpine vegetation. The remaining vegetation types were labeled as 'others' (figure 1).

2.2. Index selection

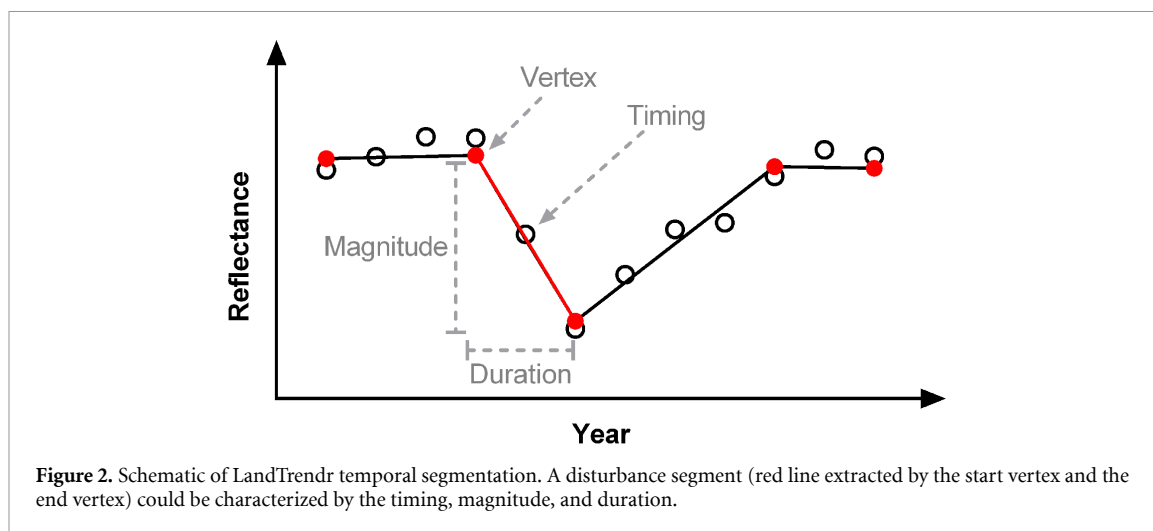
An analysis of six spectral indices was carried out in order to determine which one captures the variation in time series most accurately: the normalized burn ratio (NBR), the normalized difference vegetation index (NDVI), normalized difference moisture index (NDMI), and the tasseled cap transformation indices greenness (TCG), brightness (TCB) and wetness (TCW). The analysis consists of two parts, first, we chose a disturbed area covered with different vegetation (forest, meadow, and shrub) to evaluate the

sensitivity of the spectral indices at pre-disturbance, during-disturbance, and post-disturbance based on the annual composites derived from the preprocessing (Runge *et al* 2022), and it is presented in figure 1 with a size of 0.15 M ha; second, we calculated the disturbance signal-to-noise ratio (DSNR) at pixel-level on the selected area for each spectral index, which is a fit metric used to evaluate spectral index's effectiveness in disturbance detection (Cohen *et al* 2018). Higher DSNR values indicate higher signal corresponding to noise:

$$DSNR = \frac{\bar{y}_n - \bar{y}_1}{\sqrt{\frac{\sum_{i=1}^n (\bar{y}_i - \bar{y}_i)^2}{n}}} \quad (1)$$

where \bar{y}_1 and \bar{y}_n respectively represent the values of the start and end vertices of the segment; \bar{y}_i represents the fitted spectral value and y_i represents the original spectral value for all fitted points between the start vertex and end vertex. The box-plot was used to displayed different discriminating power (pre-disturbance, during-disturbance, and post-disturbance) of indices and the distribution of DSNR values for different indices.

Specially, our algorithm and analysis only focused on 'vegetated regions', which hereinafter are defined



as the pixels with an average NDVI larger than 0.1 over all growing seasons.

2.3. Time-series segmentation process

The pre-processed time series data were applied as input to the temporal segmentation algorithm, LandTrendr (Kennedy *et al* 2010). It is a spectral-temporal segmentation algorithm which is used to detect change in a time series of moderate resolution satellite imagery for producing trajectory-based spectral time series information. This generated a set of annual fitted images and a series of vertices bounding line segments (SI appendix, The process of LandTrendr temporal segmentation). According to the segmented trajectories, we further utilized several disturbance attributes (figure 2): timing of disturbance is defined as the first year in which the disturbance is visible; magnitude of disturbance is defined as the difference between the spectral value corresponding to the onset vertex and that corresponding to the ending vertex; duration of disturbance is defined as the time span (in years) of the segment (Kennedy *et al* 2012).

2.4. Disturbance change mapping

In this study, we applied the standard LandTrendr parameters for segmentation and fitting processes. Because of the concerns towards the forest management unit, much forest-related research set thresholds for both the mapping unit and disturbance magnitude (e.g. Griffiths *et al* 2012, Kennedy *et al* 2012). However, in order to maximize sensitivity in detecting vegetation change, we did not limit the mapping unit and disturbance magnitude for the mapping of vegetation disturbance times in the first part of the analysis (Saura 2002). Furthermore, we defined the disturbances with area greater than 0.9 ha and magnitude over 0.2 as large-scale disturbance referring to forest-related studies (Griffiths *et al* 2012, Hislop *et al* 2019). To present the characterization of the large-scale vegetation disturbances, we picked the maximum change segment from each pixel's LandTrendr

trajectory and implemented a set of spatial filters, including setting a minimum mapping unit of 0.9 ha (10 pixels) and setting a minimum magnitude of disturbance of 0.2. We found that there was an obvious difference in the distribution of early and late stages, and therefore divided the analysis into three categories, including the results of the whole period (i.e. 1986–2018), the results before 2002 (midpoint of the whole period), and the results after 2002. From these segments that LandTrendr detected, our study resulted in a set of metrics which depict the timing, magnitude, and duration of the changes in vegetation.

2.5. Accuracy assessment

2.5.1. Sampling procedure

To validate the vegetation disturbance map, we built a stratified random sample set, including 918 pixels for undisturbed vegetation and 432 pixels for disturbance class (SI appendix, figure S3), which was determined following the sampling design suggested by Olofsson *et al* (2014). We also conducted a field survey towards 100 points (68 for undisturbed area and 32 for disturbed areas) in 2020. All samples were manually interpreted by independent interpreters through TimeSync⁷, combined with very high resolution (VHR) imageries accessible in Google Earth and some other satellite-borne VHR imageries, like QuickBird (0.61 m), WorldView (0.3–0.5 m), and RapidEye (5 m) (Cohen *et al* 2010). Since some samples cannot be labeled because of data gaps, a total of 1353 samples (496 samples for disturbance and 857 disturbance samples for no disturbance) remained for accuracy assessment.

2.5.2. Accuracy analysis

The accuracies of the final disturbance map were assessed using 1353 pixel-based interpreted samples. The accuracies were evaluated with regard to overall accuracy (OA) according to the sample count-based

⁷ <https://github.com/eMapR/TimeSync-Legacy>

error matrix following the method suggested by Olofsson *et al* (2014). The class-specific omission error, commission error and F1 score were also calculated based on the error matrix. To evaluate the accuracy of detected disturbance onset, we compared the detected disturbance years (i.e. the disturbance onset assigned by the algorithm) versus the interpreted disturbance years (i.e. the disturbance onset assigned by the manual interpretation) in the validation data. In addition, we inspected two temporal segmentations for two examples to perform qualitative analysis.

2.6. Analysis of the potential agents for the vegetation disturbance change

Considering the spatial distribution of the large-scale disturbances after 2002, we used the points from field survey to explore the potential agents for the large-scale vegetation disturbance and further selected five typical areas to inspect the disturbance agents. The agent was divided into three categories, including anthropogenic factor (e.g. urbanization and road construction), natural factor (e.g. fire and earthquake), and others. To comprehensively examine the historical change and change agents, we employed multiple data resources for disturbance characterization, including the statistical yearbook, local history raw Landsat data, and other available satellite images (i.e. QuickBird, WorldView, and RapidEye).

3. Results

3.1. The best performed index for disturbance mapping

The results suggest that the NBR, NDVI, and NDMI had the highest discriminating power between the three stages in their respective time series (figure 3). The NDVI and NDMI exhibited the most marked differences between the three stages, while the changes in the NBR was relatively minor. Besides, the DSNR distribution presents that the NDVI have a higher distribution of DSNR compared to that of the NDMI, showing a better performance for detecting vegetation disturbance. Although the indices as NBR are broadly regarded as better at describing forest structure than the indices using shorter wavelengths (e.g. the ever-present NDVI) (Hislop *et al* 2018), the NDVI is less sensitive than other indices to varying sun-sensor geometry, hence making a NDVI a safe and robust option for time-series analyses (Veraverbeke *et al* 2012, Morton *et al* 2014); in addition, most vegetation types in the TP belong to the species with relatively low biomass. In the case of low vegetation biomass, NDVI performs better than those shortwave-infrared based indices (e.g. NBR and NDMI) which are sensitive to variations in the forest structure (Cohen and Goward 2004, Cuevas-gonzález *et al* 2009, Gasparri *et al* 2010), by avoiding common

saturation problem. The NDVI was therefore selected as the input for temporal segmentation.

3.2. The accuracy of disturbance mapping

After taking the potential bias derived from the stratified sampling design into consideration, our disturbance mapping obtained an OA of 81.15% (table 1). Disturbance commission and omission errors were 21.10% and 33.67%, respectively. As for the undisturbed class, the commission and omission errors were 17.84% and 10.27%, respectively. The F1 score of accuracy assessment reached 0.72, which indicated that the LandTrendr performed well in capturing the vegetation disturbances. Figure 4 displayed that most samples are distributed on or near the 1:1-line, suggesting that the onsets of disturbances have been correctly assigned. The qualitative analysis demonstrated that the breaks and the trends identified from temporal segmentation align well with what we observed from the ground (SI appendix, figure S4).

3.3. Disturbance maps and its spatial and temporal characteristics over the TP

The disturbance distribution and frequency are mapped in figure 5. We identified a total of 75.71 M ha of vegetation disturbance across the TP over the period of 1986–2018, which accounts for 29.34% of TP's area. In all vegetated areas, most have not been disturbed ($count = 0$, 69.6%, figure 5(E)). Within the disturbed vegetation areas, vegetation disturbance occurred mainly for 1–3 times, and they were evenly distributed in the TP. Also, the areas with a single disturbance were dominated, accounting for a proportion of 22.8% of TP's area. The disturbed area was widely distributed in the vegetated area while the distribution was relatively dense in the following areas: the areas around the cities, like Sining (figure 5(A)), Lhasa, and Nyingchi (figure 5(B)); the southern edges of the TP where the land was covered with dense forests (figure 5(C)) were also suffered from a higher disturbance frequency; the eastern edges of the TP with high forest coverage which was once devastated by a major earthquake in 2008 (figure 5(D)). Figure 6 presents the area of vegetation disturbed by year, and an average of 2.29 M ha of vegetation has experienced disturbance per year. Apart from the year 1988 with a relatively high disturbed areas detected (3.53×10^6 ha), the results for other years did not vary greatly. Still, an obvious increasing trend was observed from 2015 to 2018.

We further explored the characteristics of timing, magnitude, and duration of vegetation disturbance for the first, second, and third times within the study period, respectively (figure 7). As for the first time (figures 7(A), (D) and (G)), the timings of disturbances were relatively scattered throughout the vegetated areas over the TP. Specifically, the first disturbances in the central of the TP were earlier than that

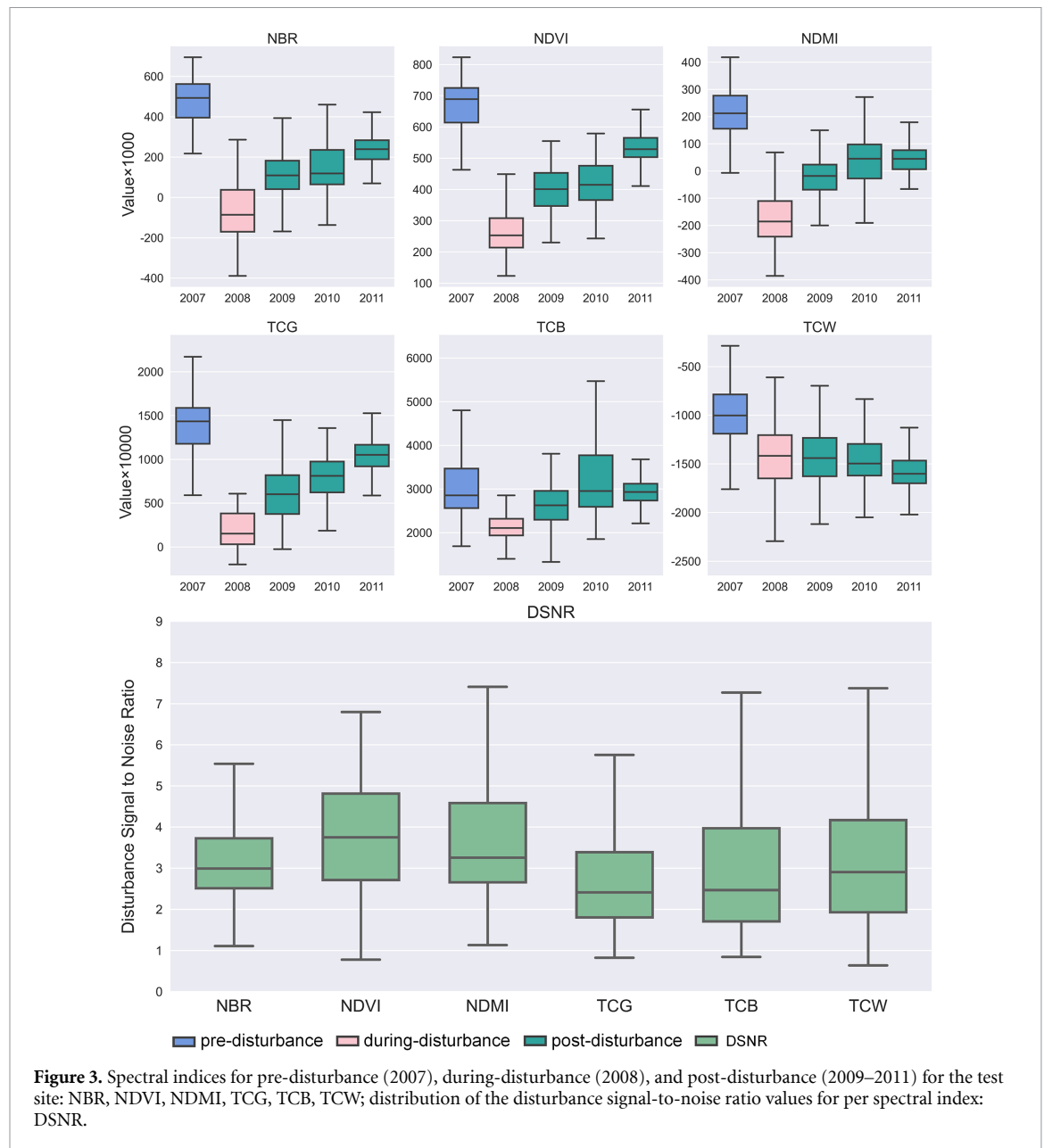


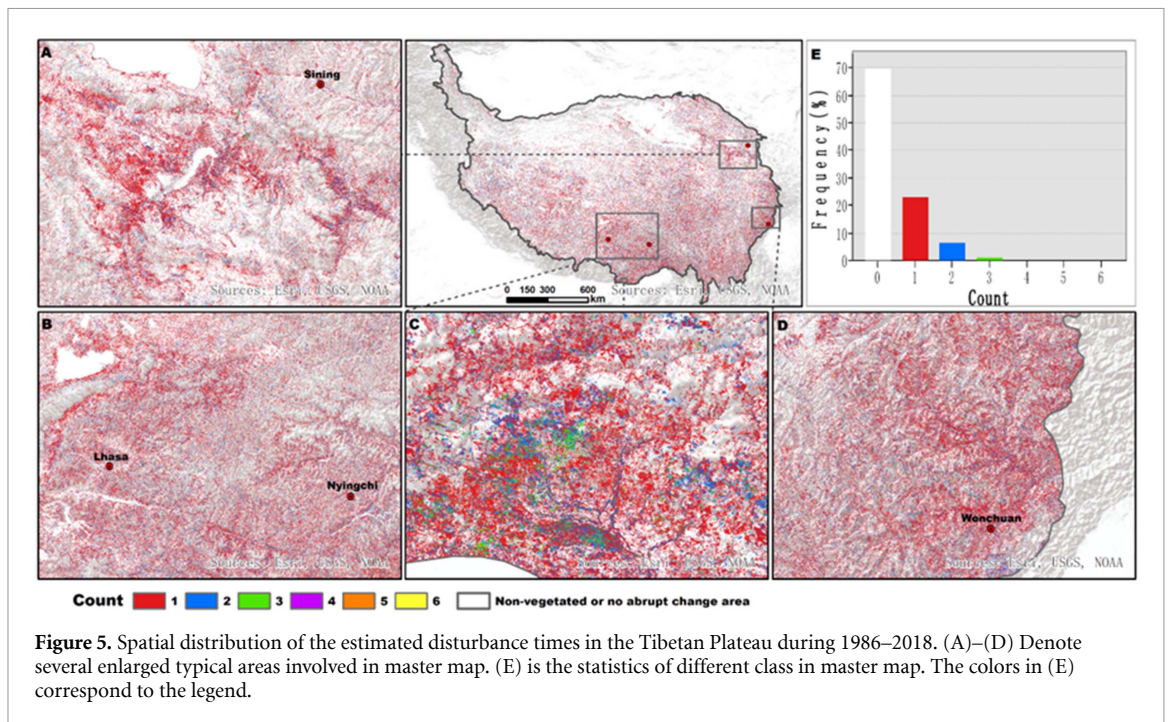
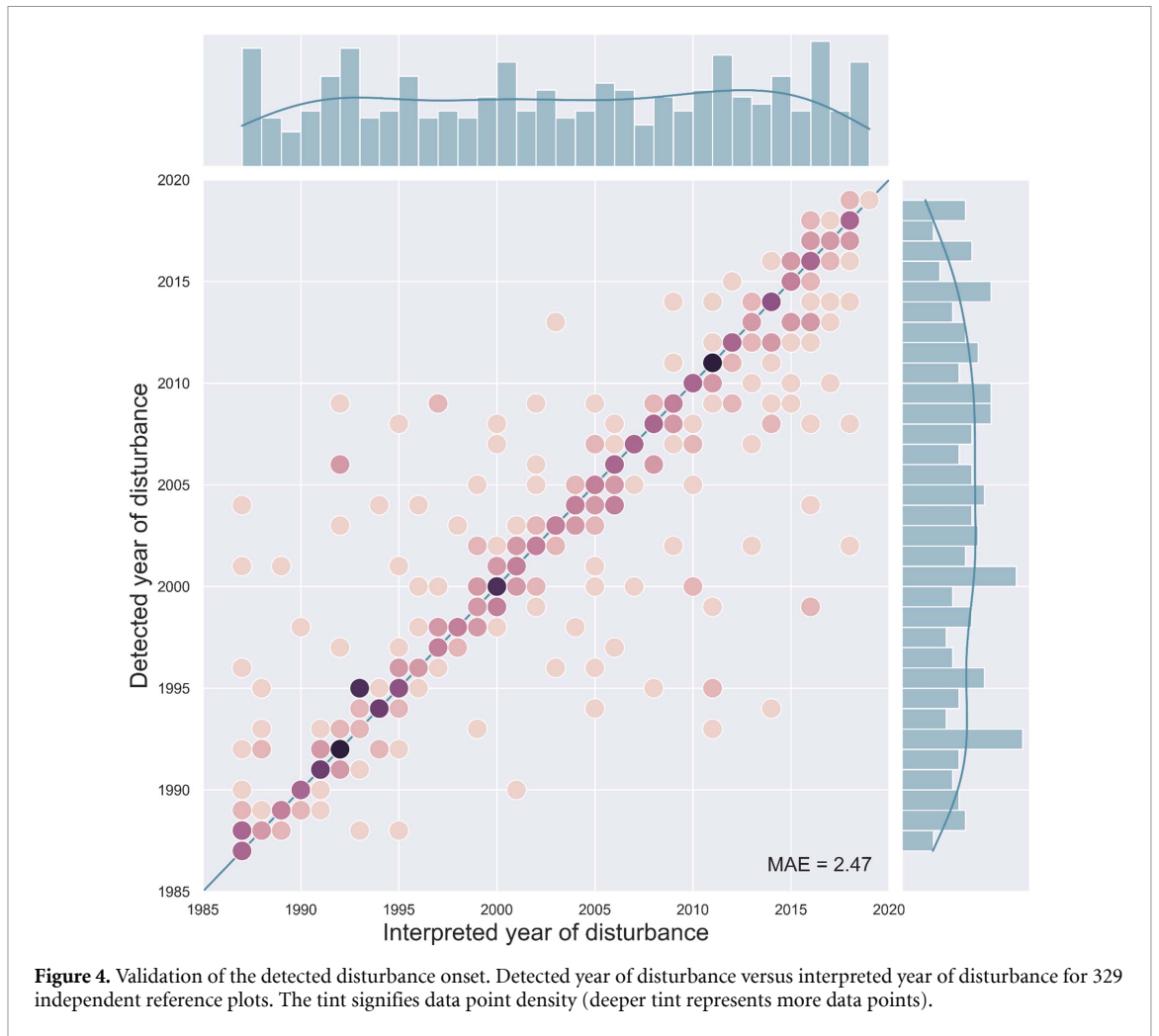
Figure 3. Spectral indices for pre-disturbance (2007), during-disturbance (2008), and post-disturbance (2009–2011) for the test site: NBR, NDVI, NDMI, TCG, TCB, TCW; distribution of the disturbance signal-to-noise ratio values for per spectral index: DSNR.

Table 1. Confusion matrix, overall accuracy, and errors of omission and commission, as well as F1 score, all derived from independent and randomly distributed validation samples of $n = 1,353$.

Estimated	Interpreted		Total	Commission error
	Disturbance	No disturbance		
Disturbance	329	88	417	21.10%
No disturbance	167	769	936	17.84%
Total	496	857	1,353	
Omission error	33.67%	10.27%		
Overall accuracy = 81.15%		F1 score = 0.72		

in the northern and southern regions of the TP; the magnitude of disturbances was mainly concentrated between 0 and 0.10, and the disturbances distributed in the southeastern TP was larger than that distributed in the northwestern TP; as for the disturbance duration, most disturbances lasted 1–5 yr distributed across the vegetated area. As for the second time (figures 7(B), (E) and (H)), the disturbance in the

central and east of the TP was earlier than that in the northern and southern edges of the TP; the results of the magnitude of the second disturbances were similar with that of the first disturbance; most second disturbances lasted 1–5 yr also while some disturbance lasted more than 16 yr, which was mainly distributed in the central and eastern TP. As for the third time (figures 7(C), (F) and (I)), the spatial pattern of



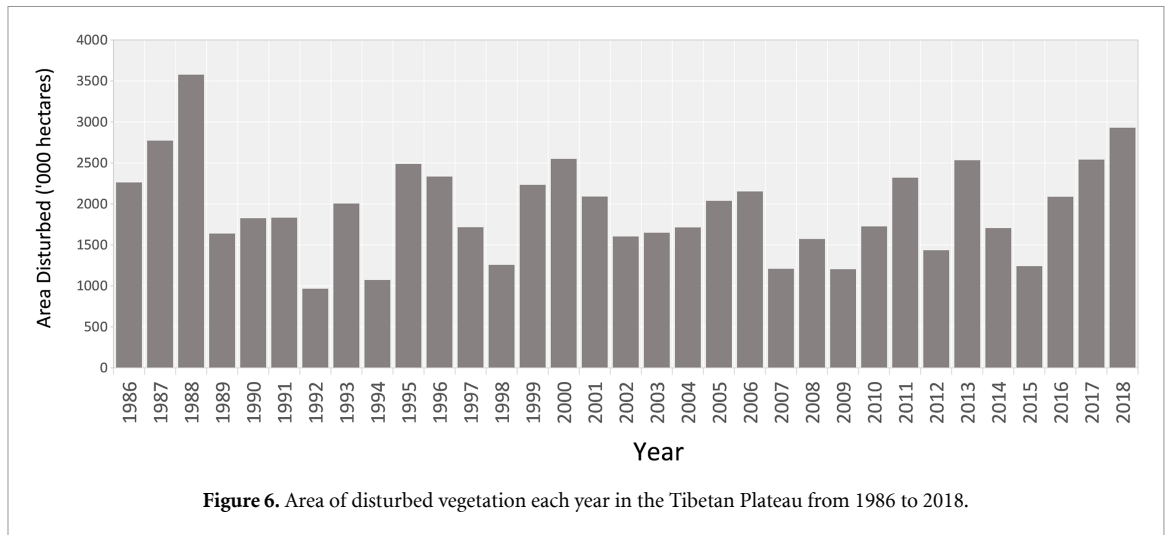


Figure 6. Area of disturbed vegetation each year in the Tibetan Plateau from 1986 to 2018.

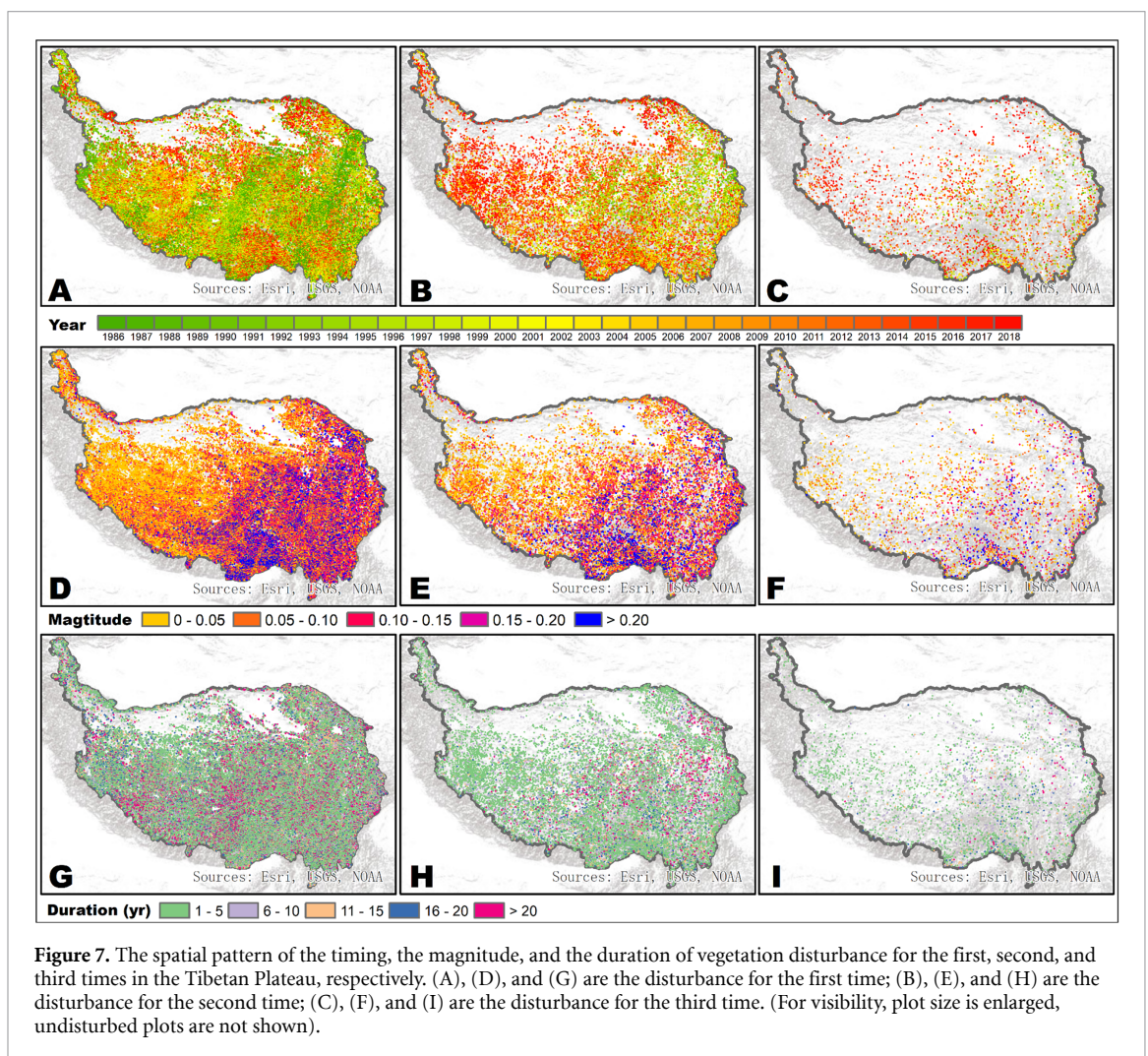


Figure 7. The spatial pattern of the timing, the magnitude, and the duration of vegetation disturbance for the first, second, and third times in the Tibetan Plateau, respectively. (A), (D), and (G) are the disturbance for the first time; (B), (E), and (H) are the disturbance for the second time; (C), (F), and (I) are the disturbance for the third time. (For visibility, plot size is enlarged, undisturbed plots are not shown).

disturbance was similar to that for the first and second times, but the disturbance pixels were much sparser.

3.4. The characteristics of large-scale disturbances

Figure 8 displays the spatial and temporal patterns of timing, magnitude, and duration of the large-scale vegetation disturbances. The timing of the disturbance of different categories (i.e. 1986–2018,

1986–2001, and 2002–2018) was obviously different between the south and north of the east-west section of the Yarlung Tsangpo river (SI appendix, figure S5) in the southeastern of the TP (figures 8(A)–(C)). Most disturbances in the north occurred early, while most in the south occurred late. Furthermore, the disturbance points were evenly distributed in the southeastern of the TP before 2002 while that were

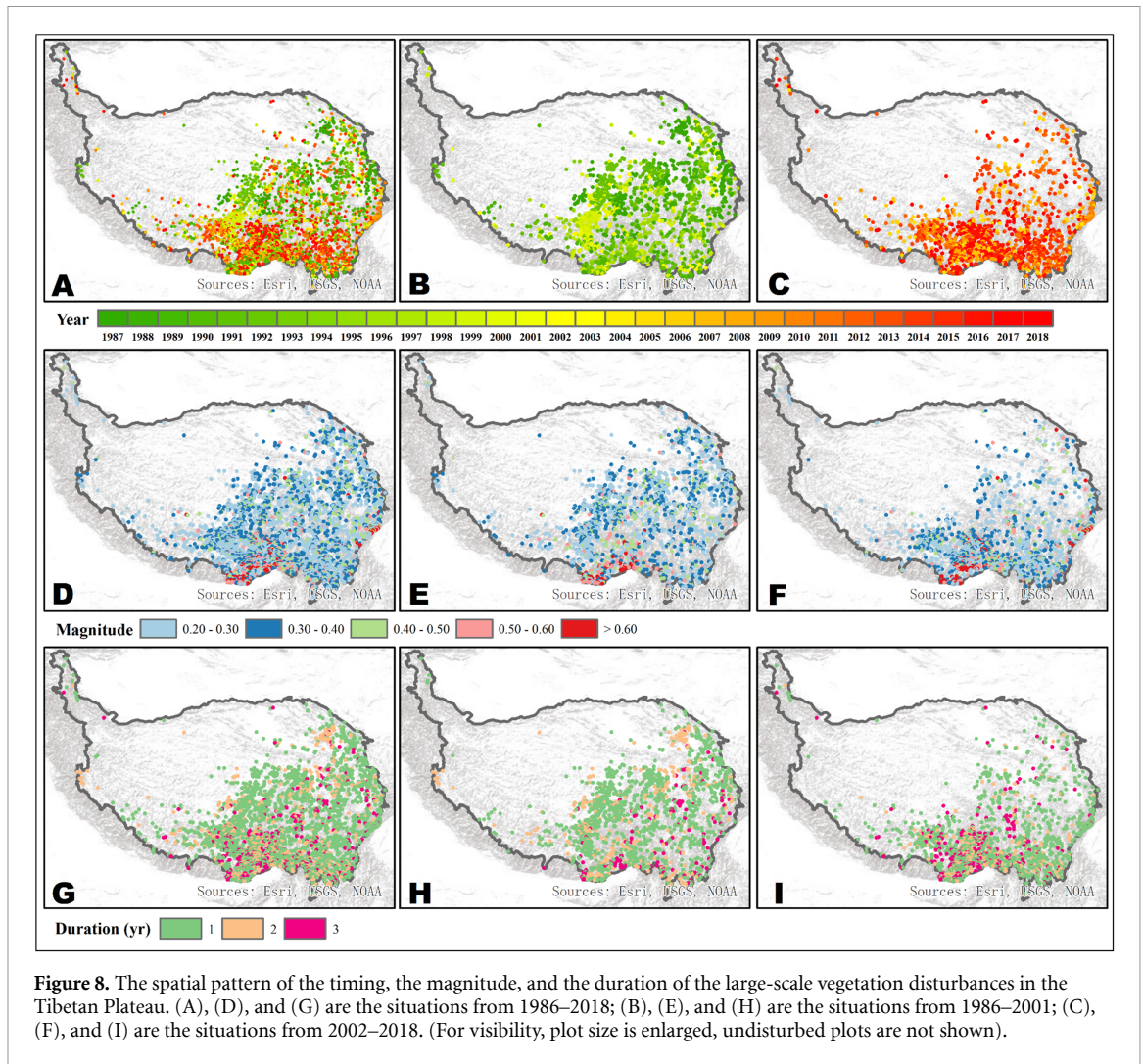


Figure 8. The spatial pattern of the timing, the magnitude, and the duration of the large-scale vegetation disturbances in the Tibetan Plateau. (A), (D), and (G) are the situations from 1986–2018; (B), (E), and (H) are the situations from 1986–2001; (C), (F), and (I) are the situations from 2002–2018. (For visibility, plot size is enlarged, undisturbed plots are not shown).

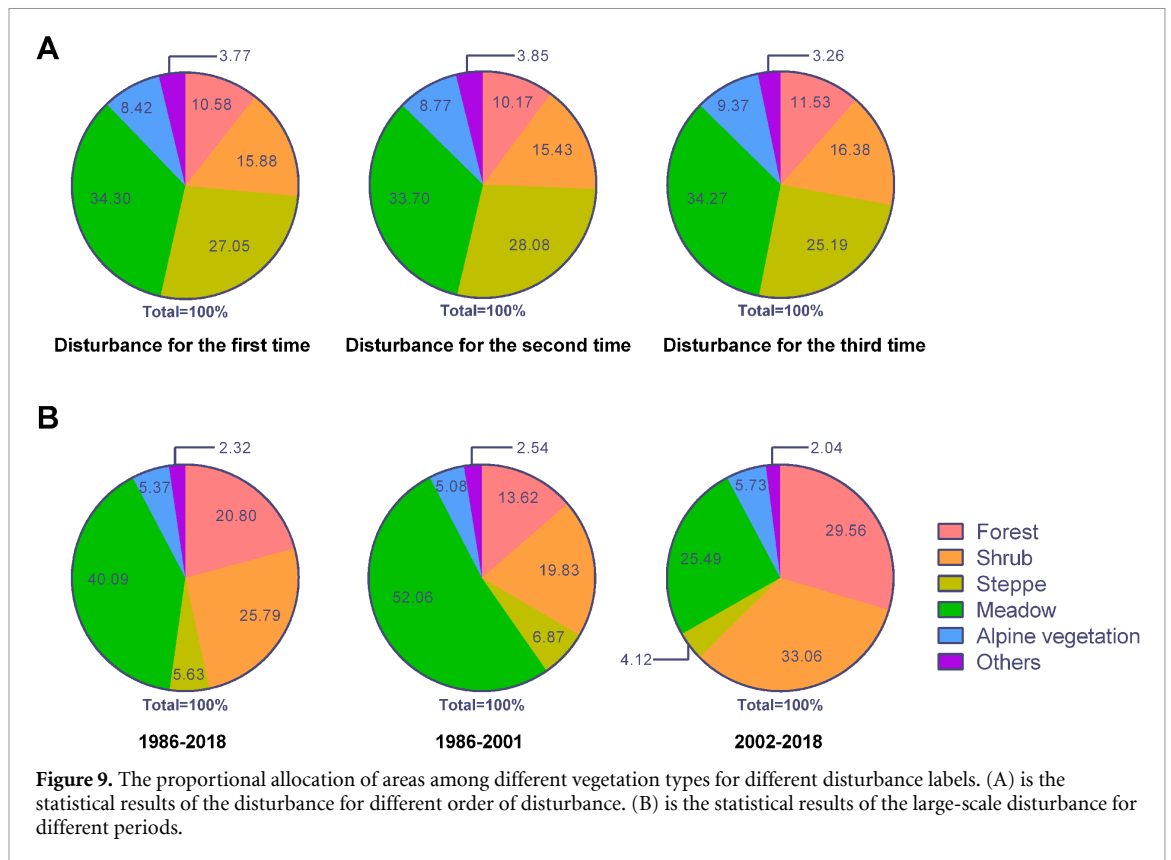
concentrated in the south of the Yarlung Tsangpo and were sparse in the north of the Yarlung Tsangpo after 2002. As for the magnitude of the disturbance of different categories (figures 8(D)–(F)), most disturbances' magnitude was 0.2–0.3 and the points were scattered in the area. Still, a few points with a relatively large disturbance magnitude (>0.5) were distributed in the southern and eastern edges of the TP (i.e. northwestern Sichuan province, China). For the duration of disturbance in different categories (figures 8(G)–(I)), most disturbances lasted one year. The disturbance points with a duration of 1–3 yr were randomly scattered throughout the area no matter for the results of 1986–2018 or the results of 1986–2001. But the results of 2002–2018 reveal that the disturbances that lasted three years were concentrated in the south of the Yarlung Tsangpo.

In summary, our results indicate that there was a noticeable difference between the situations before and after 2002 in terms of the large-scale disturbances. Specifically, the disturbances before 2002 were evenly dispersed across the southeastern TP, while the disturbances after 2002 were spatially clustered in the south of the Yarlung Tsangpo.

3.5. The distribution of vegetation disturbances among different vegetation types

Figure 9 presented the results in two parts including all disturbances (disturbance for the first, second, and third time, respectively) and the large-scale disturbances (the results of 1986–2018, 1986–2001, and 2002–2018, respectively). The disturbance distribution over different land covers are similar for the disturbances of different sequence (the first, second, and third time) (figure 9(A)), dominated by Meadow and Steppe (together over 50% of the disturbed area) and followed by Shrub, Forest, Alpine vegetation, and Others.

As shown in figure 9(B), during the whole study period (1986–2018), most large-scale disturbances happened over meadow (40.09%), followed by the shrub (25.79%) and the forest (20.80%); during the period of 1986–2002, large-scale disturbances dominated over meadow (52.06%) with substantial proportions over shrubland (19.83%) and forest (13.62%); during the period of 2001–2018, on the contrary, the disturbances occurred mostly over shrubland (33.06%) and forest (29.56%), but less over meadow (25.49%).



3.6. The potential agents for the vegetation disturbance

Among all points, 56.3% of the points induced by anthropogenic factor, 25% by natural factor, and 18.7% by others. We further chose five typical areas to inspect the agents (figure 10). Point A was within the affected region of the Lhasa-Pondo Water Control Project. The detected disturbances in this area coincide with the beginning year of the project. The detailed disturbance map shows that the timing of the main disturbances was 2014 and the outline of disturbance points is similar to the shape of the river in 2014. Point B is located between the G219 National highway and the Lhasa-Nyingchi Railway, and most disturbances here occurred in 2019. We also found that the road and the railway were under intensive construction around that year. Point C is located in the southwest of Nyingchi city, and the disturbances appeared between 2015–2018. The results suggest substantial land use change from vegetation to other types during the period. Point D is located in the northwestern Nyingchi near the G318 National highway. The main disturbances occurred in 2008, which is attributed to a forest fire. Point E is located at the eastern fringe of the TP belonging to Wenchuan County, Sichuan province. A large area of vegetation was disturbed in 2008, which is reasonable as an earthquake of magnitude 8.0 named the Wenchuan Earthquake occurred in this area.

4. Discussion

For the overall disturbance, the timings of the first and second disturbances in the central of the TP were earlier than that in the northern and southern regions of the TP. The range of these earlier disturbances is also similar to that of rangelands of the TP (Dong and Sherman 2015). Some previous studies have proved that the rangelands of the central TP have been overexploited by local pastoralists (Dong *et al* 2011). Therefore, these earlier disturbances may be because large areas of grazed grassland (steppe and meadow) in the central of the TP, and the vegetation have been disturbed due to the overgrazing in the early years.

For the large-scale disturbances, it is intriguing that the disturbance locations were evenly distributed in the southeastern of the TP before the 21st century, while the disturbance points were concentrated in the south of the Yarlung Tsangpo and were sparse in the north of the Yarlung Tsangpo after the 21st century.

The uniform and wide distribution of the disturbance areas over meadow before 21st century (figure 8(B)) was probably caused by overgrazing. Many previous studies have reported that the TP's grasslands were under degradation in recent decades (Wang *et al* 2005, Dong *et al* 2013), which might be largely attributed to a combination of overstocking beyond carrying capacity and unscientific livestock

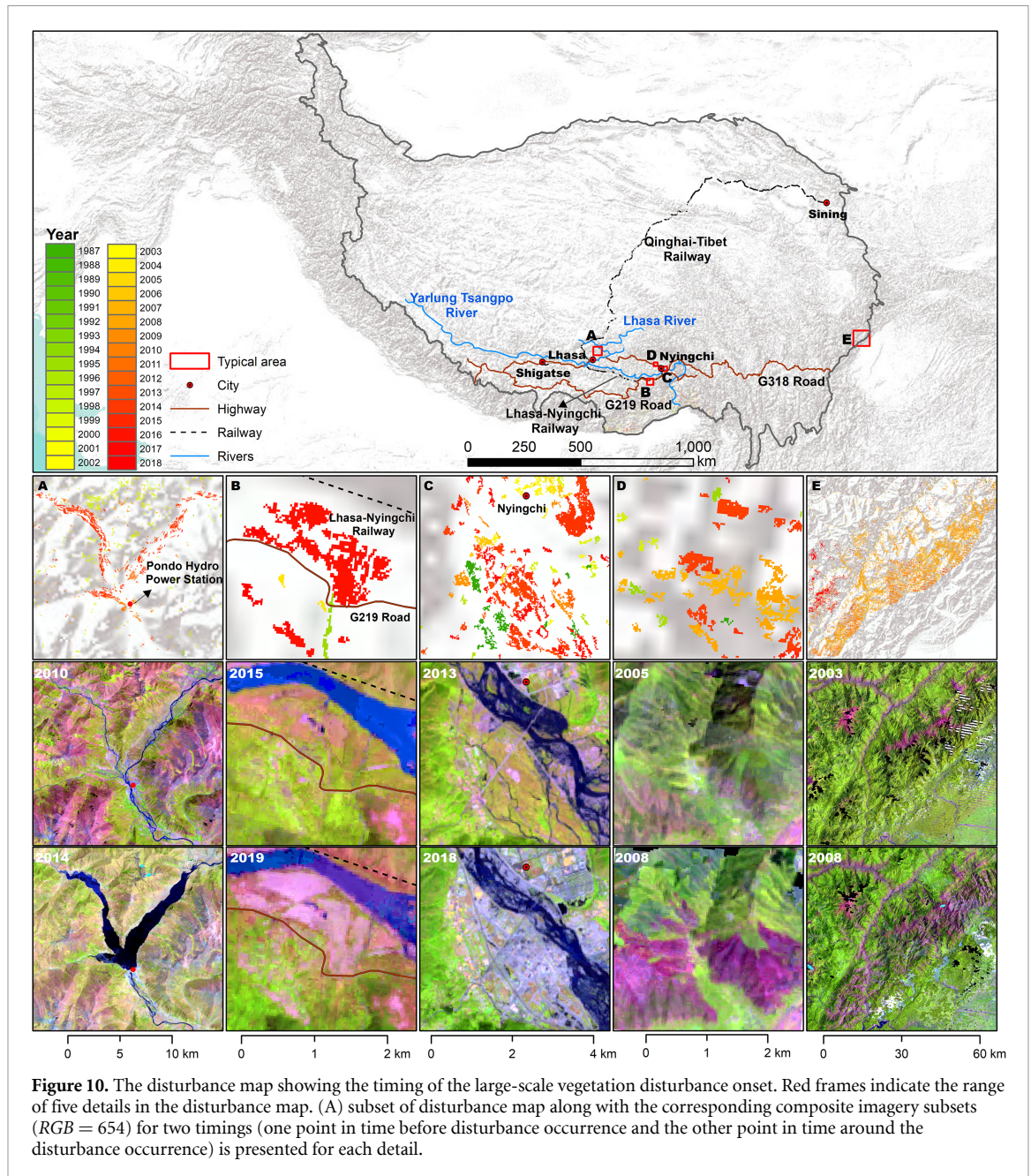


Figure 10. The disturbance map showing the timing of the large-scale vegetation disturbance onset. Red frames indicate the range of five details in the disturbance map. (A) subset of disturbance map along with the corresponding composite imagery subsets ($RGB = 654$) for two timings (one point in time before disturbance occurrence and the other point in time around the disturbance occurrence) is presented for each detail.

management (Li 1994, Wang 1999). After entering the 21st century, a range of ecological restoration projects (e.g. The Grain for Green Project, Grazing Withdrawal Program, and others) have been enforced across the TP (Li et al 2016). These projects have shown their effectiveness in facilitating the restoration of vegetation cover, coincident with the diminished frequency of the disturbances in the meadow found in this study (figure 9(B)) and the sparse distribution of disturbances in the north of the Yarlung Tsangpo after 2002 (figure 8(C)).

The distribution of the large-scale vegetation disturbances among different vegetation types indicated that the disturbances occurred more frequently in the meadow in the early period, while in the late period, there is a decreased disturbance in the meadow areas with an increased disturbance observed in forest and

Table 2. Statistics of different items in Tibet in different years.

	Total amount				
	2000	2005	2010	2015	2020
Hydroelectric power (10^8 kWh)	5.54	12.10	15.85	39.51	70.24
Length of highways (km)	22 503	43 716	60 810	78 348	118 831
Length of rail lines (km)	0	531	531	786	786
Urbanization rate (%)	19.47	20.85	22.67	27.74	32.00

shrub areas. The meadow is an important part of the rangeland on the TP, accounting for 44.64% of the area (Jian 2002). Therefore, a possible explanation is that the local economy was highly dependent on

grazing before the 21st century; however, after the 21st century, local residents became less dependent on livestock husbandry and started to interfere with the forest and shrub more frequently due to the increasing demand for wood in the context of urbanization. For instance, the Tibet's industrial structure has been changing after entering the 21st century: the ratio of the primary industry has decreased gradually while an increase in the ratio of the secondary industry has been observed, showing a pattern with tertiary in the lead, secondary industry as the middle, and primary industry as the smallest one; along with the development of the economy, many labors from the primary industry have transferred to the other industries (Tibet Bureau of Statistics 2020).

We further analyzed five typical areas to inspect the disturbance agents. Main disturbances in five areas were caused by anthropogenic factors (i.e. the construction of hydro power station, the construction of highway and railway, urbanization) and natural hazards (i.e. forest fire and earthquake). Moreover, most disturbance sites are found in the triangle area formed by the Lhasa, Shigatse, and Nyingchi, which is the most economically active region on the TP in the 21st century. In general, economic development is always accompanied by intensive human activities, such as highway or railway construction, urban expansion, and water conservancy project. Roads are one of humankind's most productive linear infrastructures, driving habitat transformation directly (Trombulak and Frissell 2000). Especially, the timings of disturbances in point B were within the period of the construction of the G219 National highway and the Lhasa–Nyingchi Railway, and the vegetation was therefore more likely be disturbed by these projects. Li *et al* (2013) also demonstrated the areas along the traffic arteries that are exposed to frequent human activities had suffered severe degradation on the TP. Many related studies revealed that the impoundment of the reservoir has a great influence on the growth of riparian vegetation (Li *et al* 2015, Botelho *et al* 2017). Also, hydropower dams may also fragment habitat, reduce the distribution of primary vegetation, and simplify the types of vegetation along the rivers (Li *et al* 2012). These factors may explain the occurrence of concentrative disturbances in point A. As for the urbanization, although it plays a central role in economic growth and social development, it also profoundly alters the physical environment far beyond city range, leading to habitat loss, vegetation degradation (Chen 2007). Over the last two decades, Tibet has been witnessing a dramatic growth of economy like many other cities in China. As table 2 shows, there has been a dramatic rise in the number of several significant indicators of economic development, including hydroelectric power, length of highways, length of rail lines, and urbanization rate. We also found that there is an increasing trend with the area of disturbed vegetation each year from 2015 to 2018

when these indicators showed an apparent increase. These further proved that the growth of vegetation has been affected by anthropogenic activities to varying degrees along with rapid economic growth.

Although a high-resolution map of vegetation disturbance was obtained, there are still some limitations regarding the data and method. Firstly, cloud cover was an inherent issue over the TP, especially in the southeastern TP (figure 3). In contrast to the conterminous United States, the data density of Landsat archive in the TP is so far substantially lower (Wulder *et al* 2016). These factors considerably limit the acquisition of cloud-free Landsat observations, which further increases the difficulties for extracting accurate disturbance information from time-series datasets. Multisensor analysis may potentially alleviate data density issues but could also introduce uncertainties during the data fusion process (Roy *et al* 2016). Secondly, we were not able to distinguish the disturbance agents for all individual disturbance patch, because there were not adequate agent-specific training data. Future work is warranted to develop disturbance agent algorithms and map products, which will provide a more comprehensive examination of disturbance drivers for the TP region. Despite these limitations, this work provides important baseline disturbance information, which laid a solid foundation for further investigating the relationship between vegetation growth and anthropogenic activities over the last decades across the TP in future.

5. Conclusion

In this study, the spatiotemporal patterns of vegetation disturbance across the TP were investigated based on the LandTrendr algorithm using 30 m Landsat archives for the period of 1986–2018. The results demonstrated that the disturbances in vegetated land have been existing in the context of vegetation greening across the TP over the last decades. During 1986–2018, 75.71 M ha (accounting for 29.34% of TP's area) of vegetated area was disturbed, of which 8.44 M ha area experienced large-scale disturbances. The disturbances were dominated in meadow areas, largely attributed to a combination of overstocking and livestock mismanagement before 2002. Along with the implementation of several policies regarding ecology conservation around 2002, the disturbances in the meadow have diminished. Instead, most vegetation disturbances were gathered in the south of the Yarlung Tsangpo after 2002 which was mainly induced by anthropogenic activities such as urbanization, the construction of roadways and railway, fire hazards, and water control projects. These emerging threats may bring about unexpected changes in TP's ecology in the future. Our work provides critical insights into vegetation variation over the TP during

the past 40 yr, which are essential for development planning and environmental management.

Data availability statement

The data that support the findings of this study are available upon reasonable request from the authors.

Acknowledgments

This work was funded by the National Natural Science Foundation of China Key Projects (No. 41930754), the Second Tibetan Plateau Scientific Expedition and Research (STEP) program (No. 2019QZKK0105), and the National Natural Science Foundation of China (No. 32060370).

Conflict of interest

The authors declare that they have no known competing financial interests or personal relationships that could have appeared to influence the work reported in this paper.

ORCID iDs

Yanyu Wang  <https://orcid.org/0000-0002-5369-6860>

Jinfeng Chang  <https://orcid.org/0000-0003-4463-7778>

Zhou Shi  <https://orcid.org/0000-0003-3914-5402>

References

- Banskota A, Kayastha N, Falkowski M J, Wulder M A, Froese R E and White J C 2014 Forest monitoring using Landsat time series data: a review *Can. J. Remote Sens.* **40** 362–84
- Bonan G B, Pollard D and Thompson S L 1992 Effects of boreal forest vegetation on global climate *Nature* **359** 716–8
- Botelho A, Ferreira P, Lima F, Pinto L M C and Sousa S 2017 Assessment of the environmental impacts associated with hydropower *Renew. Sustain. Energy Rev.* **70** 896–904
- Brun P, Zimmermann N E, Graham C H, Lavergne S, Pellissier L, Münkemüller T and Thuiller W 2019 The productivity-biodiversity relationship varies across diversity dimensions *Nat. Commun.* **10** 1–11
- Bullock E L, Woodcock C E and Holden C E 2020 Improved change monitoring using an ensemble of time series algorithms *Remote Sens. Environ.* **238** 111165
- Ceccherini G, Duveiller G, Grassi G, Lemoine G, Avitabile V, Pilli R and Cescatti A 2020 Abrupt increase in harvested forest area over Europe after 2015 *Nature* **583** 72–77
- Chen H, Zhu Q, Peng C, Wu N, Wang Y, Fang X, Gao Y, Zhu D, Yang G and Tian J 2013 The impacts of climate change and human activities on biogeochemical cycles on the Qinghai-Tibetan Plateau *Glob. Change Biol.* **19** 2940–55
- Chen J 2007 Rapid urbanization in China: a real challenge to soil protection and food security *Catena* **69** 1–15
- Chen Y, Feng X, Tian H, Wu X, Gao Z, Feng Y and Fu B 2021 Accelerated increase in vegetation carbon sequestration in China after 2010: a turning point resulting from climate and human interaction *Glob. Change Biol.* **27** 5848–64
- Cohen W B and Goward S N 2004 Landsat's role in ecological applications of remote sensing *Bioscience* **54** 535–45
- Cohen W B, Yang Z, Healey S P, Kennedy R E and Gorelick N 2018 A LandTrendr multispectral ensemble for forest disturbance detection *Remote Sens. Environ.* **205** 131–40
- Cohen W B, Yang Z and Kennedy R 2010 Detecting trends in forest disturbance and recovery using yearly Landsat time series: 2. TimeSync—tools for calibration and validation *Remote Sens. Environ.* **114** 2911–24
- Cuevas-gonzález M A R Í A, Gerard F, Balzter H and Riano D 2009 Analysing forest recovery after wildfire disturbance in boreal Siberia using remotely sensed vegetation indices *Glob. Change Biol.* **15** 561–77
- DeFries R, Field C, Fung I, Collatz G and Bounoua L 1999 Combining satellite data and biogeochemical models to estimate global effects of human-induced land cover change on carbon emissions and primary productivity *Glob. Biogeochem. Cycles* **13** 803–15
- Dixon R K, Solomon A, Brown S, Houghton R, Trexler M and Wisniewski J 1994 Carbon pools and flux of global forest ecosystems *Science* **263** 185–90
- Dong Q-M, Zhao X-Q, Wu G-L, Shi -J-J and Ren G-H 2013 A review of formation mechanism and restoration measures of “black-soil-type” degraded grassland in the Qinghai-Tibetan Plateau *Environ. Earth Sci.* **70** 2359–70
- Dong S and Sherman R 2015 Enhancing the resilience of coupled human and natural systems of alpine rangelands on the Qinghai-Tibetan Plateau *Rangel. J.* **37** i–iii
- Dong S, Wen L, Liu S, Zhang X, Lassoie J P, Yi S, Li X, Li J and Li Y 2011 Vulnerability of worldwide pastoralism to global changes and interdisciplinary strategies for sustainable pastoralism *Ecol. Soc.* **16** 10
- Flood N 2013 Seasonal composite Landsat TM/ETM+ images using the medoid (a multi-dimensional median) *Remote Sens.* **5** 6481–500
- Gasparri N I, Parmuchi M G, Bono J, Karszenbaum H and Montenegro C L 2010 Assessing multi-temporal Landsat 7 ETM+ images for estimating above-ground biomass in subtropical dry forests of Argentina *J. Arid Environ.* **74** 1262–70
- Griffiths P, Kuemmerle T, Kennedy R E, Abrudan I V, Knorn J and Hostert P 2012 Using annual time-series of Landsat images to assess the effects of forest restitution in post-socialist Romania *Remote Sens. Environ.* **118** 199–214
- Haberl H, Erb K H, Krausmann F, Gaube V, Bondeau A, Plutzer C, Gingrich S, Lucht W and Fischer-Kowalski M 2007 Quantifying and mapping the human appropriation of net primary production in earth's terrestrial ecosystems *Proc. Natl Acad. Sci.* **104** 12942–7
- Hansen M C, Krylov A, Tyukavina A, Potapov P V, Turubanova S, Zutta B, Ifo S, Margono B, Stolle F and Moore R 2016 Humid tropical forest disturbance alerts using Landsat data *Environ. Res. Lett.* **11** 034008
- Hansen M C, Potapov P V, Moore R, Hancher M, Turubanova S A, Tyukavina A, Thau D, Stehman S V, Goetz S J and Loveland T R 2013 High-resolution global maps of 21st-century forest cover change *Science* **342** 850–3
- Harris R B 2010 Rangeland degradation on the Qinghai-Tibetan plateau: a review of the evidence of its magnitude and causes *J. Arid Environ.* **74** 1–12
- Healey S P et al 2018 Mapping forest change using stacked generalization: an ensemble approach *Remote Sens. Environ.* **204** 717–28
- Hislop S, Jones S, Soto-Berelov M, Skidmore A, Haywood A and Nguyen T H 2018 Using Landsat spectral indices in time-series to assess wildfire disturbance and recovery *Remote Sens.* **10** 460
- Hislop S, Jones S, Soto-Berelov M, Skidmore A, Haywood A and Nguyen T H 2019 A fusion approach to forest disturbance mapping using time series ensemble techniques *Remote Sens. Environ.* **221** 188–97
- Hou X 2019 1:1 million vegetation map of China (National Tibetan Plateau Data Center)
- Huang C, Goward S N, Masek J G, Thomas N, Zhu Z and Vogelmann J E 2010 An automated approach for

- reconstructing recent forest disturbance history using dense Landsat time series stacks *Remote Sens. Environ.* **114** 183–98
- Jian N 2002 Carbon storage in grasslands of China *J. Arid Environ.* **50** 205–18
- Kennedy R E, Yang Z and Cohen W B 2010 Detecting trends in forest disturbance and recovery using yearly Landsat time series: 1. LandTrendr—temporal segmentation algorithms *Remote Sens. Environ.* **114** 2897–910
- Kennedy R E, Yang Z, Cohen W B, Pfaff E, Braaten J and Nelson P 2012 Spatial and temporal patterns of forest disturbance and regrowth within the area of the Northwest Forest Plan *Remote Sens. Environ.* **122** 117–33
- Krawchuk M A, Meigs G W, Cartwright J M, Coop J D, Davis R, Holz A, Kolden C and Meddens A J 2020 Disturbance refugia within mosaics of forest fire, drought, and insect outbreaks *Front. Ecol. Environ.* **18** 235–44
- Li J, Dong S, Yang Z, Peng M, Liu S and Li X 2012 Effects of cascade hydropower dams on the structure and distribution of riparian and upland vegetation along the middle-lower Lancang-Mekong River *For. Ecol. Manage.* **284** 251–9
- Li M 1994 Characteristics and rational exploitation of Tibet's land resources *J. Nat. Resour.* **9** 51–57
- Li Q, Zhang C, Shen Y, Jia W and Li J 2016 Developing trend of Aeolian desertification in China's Tibet autonomous region from 1977 to 2010 *Environ. Earth Sci.* **75** 1–12
- Li X-L, Gao J, Brierley G, Qiao Y-M, Zhang J and Yang Y-W 2013 Rangeland degradation on the Qinghai-Tibet Plateau: implications for rehabilitation *Land Degrad. Dev.* **24** 72–80
- Li X, Zhang J and Xu L 2015 An evaluation of ecological losses from hydropower development in Tibet *Ecol. Eng.* **76** 178–85
- Morton D, Nagol J, Carabajal C, Rosette J, Palace M, Cook B, Vermote E, Harding D and North P 2014 Amazon forests maintain consistent canopy structure and greenness during the dry season *Nature* **506** 221
- Olofsson P, Foody G M, Herold M, Stehman S V, Woodcock C E and Wulder M A 2014 Good practices for estimating area and assessing accuracy of land change *Remote Sens. Environ.* **148** 42–57
- Parmesan C and Yohe G 2003 A globally coherent fingerprint of climate change impacts across natural systems *Nature* **421** 37–42
- Piao S, Nan H, Huntingford C, Ciais P, Friedlingstein P, Sitch S, Peng S, Ahlström A, Canadell J G and Cong N 2014 Evidence for a weakening relationship between interannual temperature variability and northern vegetation activity *Nat. Commun.* **5** 1–7
- Piao S, Wang X, Ciais P, Zhu B, Wang T A O and Liu J I E 2011 Changes in satellite-derived vegetation growth trend in temperate and boreal Eurasia from 1982 to 2006 *Glob. Change Biol.* **17** 3228–39
- Piao S, Wang X, Park T, Chen C, Lian X, He Y, Bjerke J W, Chen A, Ciais P and Tømmervik H 2020 Characteristics, drivers and feedbacks of global greening *Nat. Rev. Earth Environ.* **1** 14–27
- Qin Y, Yi S, Ren S, Li N and Chen J 2014 Responses of typical grasslands in a semi-arid basin on the Qinghai-Tibetan Plateau to climate change and disturbances *Environ. Earth Sci.* **71** 1421–31
- Qiu J 2008 China: the third pole *Nature* **454** 393–6
- Roy D P, Kovalsky V, Zhang H, Vermote E F, Yan L, Kumar S and Egorov A 2016 Characterization of Landsat-7 to Landsat-8 reflective wavelength and normalized difference vegetation index continuity *Remote Sens. Environ.* **185** 57–70
- Runge A, Nitze I and Grosse G 2022 Remote sensing annual dynamics of rapid permafrost thaw disturbances with LandTrendr *Remote Sens. Environ.* **268** 112752
- Saura S 2002 Effects of minimum mapping unit on land cover data spatial configuration and composition *Int. J. Remote Sens.* **23** 4853–80
- Senf C and Seidl R 2020 Mapping the forest disturbance regimes of Europe *Nat. Sustain.* **4** 63–70
- Shen M, Piao S, Dorji T, Liu Q, Cong N, Chen X, An S, Wang S, Wang T and Zhang G 2015a Plant phenological responses to climate change on the Tibetan Plateau: research status and challenges *Natl Sci. Rev.* **2** 454–67
- Shen M, Piao S, Jeong S-J, Zhou L, Zeng Z, Ciais P, Chen D, Huang M, Jin C-S and Li L Z X 2015b Evaporative cooling over the Tibetan Plateau induced by vegetation growth *Proc. Natl Acad. Sci.* **112** 9299–304
- Shimizu K, Ponce-Hernandez R, Ahmed O S, Ota T, Win Z C, Mizoue N and Yoshida S 2017 Using Landsat time series imagery to detect forest disturbance in selectively logged tropical forests in Myanmar *Can. J. For. Res.* **47** 289–96
- Smith T, Traxl D and Boers N 2022 Empirical evidence for recent global shifts in vegetation resilience *Nat. Clim. Change* **12** 477–84
- Tibet Bureau of Statistics 2020 *Tibet Statistical Yearbook*
- Trombulak S C and Frissell C A 2000 Review of ecological effects of roads on terrestrial and aquatic communities *Conserv. Biol.* **14** 18–30
- Veraverbeke S, Gitas I, Katagis T, Polychronaki A, Somers B and Goossens R 2012 Assessing post-fire vegetation recovery using red–near infrared vegetation indices: accounting for background and vegetation variability *ISPRS J. Photogramm. Remote Sens.* **68** 28–39
- Verbesselt J, Hyndman R, Newnham G and Culvenor D 2010 Detecting trend and seasonal changes in satellite image time series *Remote Sens. Environ.* **114** 106–15
- Wang X 1999 Sustainable use of alpine meadow grassland resource on the Qinghai-Tibet Plateau *Resour. Sci.* **21** 38–42
- Wang Y, Wang G, Shen Y and Wang Y 2005 Degradation of the eco-environmental system in alpine meadow on the Tibetan Plateau *J. Glaciol. Geocryol.* **27** 633–40
- Watts L M and Laffan S W 2014 Effectiveness of the BEAST algorithm for detecting vegetation response patterns in a semi-arid region *Remote Sens. Environ.* **154** 234–45
- Wulder M A, Loveland T R, Roy D P, Crawford C J, Masek J G, Woodcock C E, Allen R G, Anderson M C, Belward A S and Cohen W B 2019 Current status of Landsat program, science, and applications *Remote Sens. Environ.* **225** 127–47
- Wulder M A, White J C, Loveland T R, Woodcock C E, Belward A S, Cohen W B, Fosnight E A, Shaw J, Masek J G and Roy D P 2016 The global Landsat archive: status, consolidation, and direction *Remote Sens. Environ.* **185** 271–83
- Yang G, Peng C, Chen H, Dong F, Wu N, Yang Y, Zhang Y, Zhu D, He Y and Shi S 2017 Qinghai–Tibetan Plateau peatland sustainable utilization under anthropogenic disturbances and climate change *Ecosyst. Health Sustain.* **3** e01263
- Ye S, Rogan J, Zhu Z and Eastman J R 2021a A near-real-time approach for monitoring forest disturbance using Landsat time series: stochastic continuous change detection *Remote Sens. Environ.* **252** 112167
- Ye S, Rogan J, Zhu Z, Hawbaker T J, Hart S J, Andrus R A, Meddens A J, Hicke J A, Eastman J R and Kulakowski D 2021b Detecting subtle change from dense Landsat time series: case studies of mountain pine beetle and spruce beetle disturbance *Remote Sens. Environ.* **263** 112560
- Zhu Z, Piao S, Myneni R B, Huang M, Zeng Z, Canadell J G, Ciais P, Sitch S, Friedlingstein P and Arneeth A 2016 Greening of the Earth and its drivers *Nat. Clim. Change* **6** 791–5
- Zhu Z and Woodcock C E 2014 Continuous change detection and classification of land cover using all available Landsat data *Remote Sens. Environ.* **144** 152–71
- Zhu Z, Zhang J, Yang Z, Aljaddani A H, Cohen W B, Qiu S and Zhou C 2020 Continuous monitoring of land disturbance based on Landsat time series *Remote Sens. Environ.* **238** 111116